

Measurements in Particle-Laden Flows Using Magnetic Resonance Velocimetry: Time-Averaged Particle Concentration and Intrinsic Fluid Velocity

M. Bruschewski¹, W. Hogendoorn^{2,*}, D. Frank¹, W-P Breugem², C. Poelma², S. Grundmann¹

1: University of Rostock, Institute of Fluid Mechanics, Rostock, Germany

2: Delft University of Technology, Multiphase Systems, Delft, The Netherlands

* Correspondent author: W.J.Hogendoorn@tudelft.nl

Keywords: Magnetic Resonance Velocimetry, Particle-laden flow, time-averaged measurements

ABSTRACT

This study presents an experimental technique based on magnetic resonance velocimetry (MRV) for time-averaged measurements in dispersed multiphase flows. The measured variables are the intrinsic velocity field of the liquid phase and its spatial distribution, from which parameters such as particle concentration or void fraction can be calculated. There are no requirements for the optical properties, but the liquid and particles must match in terms of magnetic susceptibility in order to avoid measurement errors. Common material combinations are water-glycerol and plastic particles. Relatively low measurement uncertainty can be achieved for this technique since the measurands are intrinsically averaged throughout the data acquisition process. The sources of systematic measurement errors are well understood and errors can be reduced to a minimum. In addition, the overall accuracy of this technique can be determined after the measurement by calculating the average particle concentration and the flow rate from the MRV data. These values can be verified by the target values. Therefore, this measurement technique can serve as a ground truth for numerical studies and other experimental techniques. In this study, results are presented for a glycerol-water flow containing polystyrene particles. The investigated particle-laden flow has an average particle concentration between 10 and 50% and a Reynolds number based on the apparent suspension viscosity between 800 and 5000.

1. Introduction

Many dispersed multiphase flows are inaccessible by conventional optical techniques. A number of non-optical techniques have been developed in the past decades to provide a better insight in these flows and one of these techniques is Magnetic Resonance Velocimetry (MRV) (Poelma, 2020). MRV enables measurements of fluid velocities, species concentration and many other fluid mechanic properties in opaque flows. As a disadvantage, the temporal resolution of MRV is relatively low and usually, the relevant time-scales of the investigated turbulent flows cannot be resolved. Nonetheless, MRV can be used to generate high-quality time-averaged fluid mechanics data in single- and multiphase flows.

The signal source of the MRV data lies in the magnetic resonance of the nuclear spins. In a typical MRV experiment, only the liquid gives a measureable signal while other materials such as particles and gas bubbles are invisible to the receiver system. There is a linear dependency between the time-averaged signal magnitude and the time-averaged liquid density. Thus, the time-averaged

particle concentration can be calculated from the relative signal magnitude. The velocity data in MRV is determined from the phase angle of the received signal. In a particle-laden flow, the measured velocity represents the time-averaged intrinsic liquid velocity. Note that simultaneous measurements of particle concentration and intrinsic liquid velocity are possible.

The data are sampled in the spatial frequency domain (k-space) and only after all spatial frequencies are sampled, the data is reconstructed via an inverse fast Fourier transform (FFT). Thus, each point in the image is based on information from the entire duration of the data sampling process. The sampling duration is typically in the order of 0.1 s to 10 s for a two-dimensional acquisition and several minutes for a three-dimensional acquisition.

The time scales of the individual k-space samples are typically on the order of 1 ms. As a result, time scales in the flow that are larger than this time scale lead to deviations between the k-space samples, which appear as signal ghosts in the FFT-reconstructed image. If these deviations are uncorrelated, which is to be expected for many turbulent flows, the signal ghosts lead to random noise in the image. For this reason, the signal ghosts can be reduced by averaging several acquisitions or by filtering the data. Furthermore, statistical independence of the data sampling can also be improved by sampling the k-space in random order. The final data represent unbiased, time-averaged results with low measurement uncertainty.

2. Methods

The examined particle-laden flow contains spherical polystyrene particles in a water-glycerol fluid mixture in a pipe with diameter $D = 30.35$ mm. The average particle diameter is $d = 1.75$ mm. The density of the fluid was matched with the particle density by adding glycerol. The target water-glycerol ratio was determined based on calculations and prior experiments but extensive fine-tuning was required until neutral buoyancy was reached. The length of the pipe system was chosen to ensure fully-developed conditions. The distance between the trip ring at the outlet of the inlet chamber and the measurement position was $132 D$. Eilers's viscosity model (Eilers 1941) is used to determine the effective viscosity based on the fluid viscosity and the mean particle concentration. The Reynolds numbers in this study are based on this suspension viscosity. Figure 1 shows the setup of the experiment.

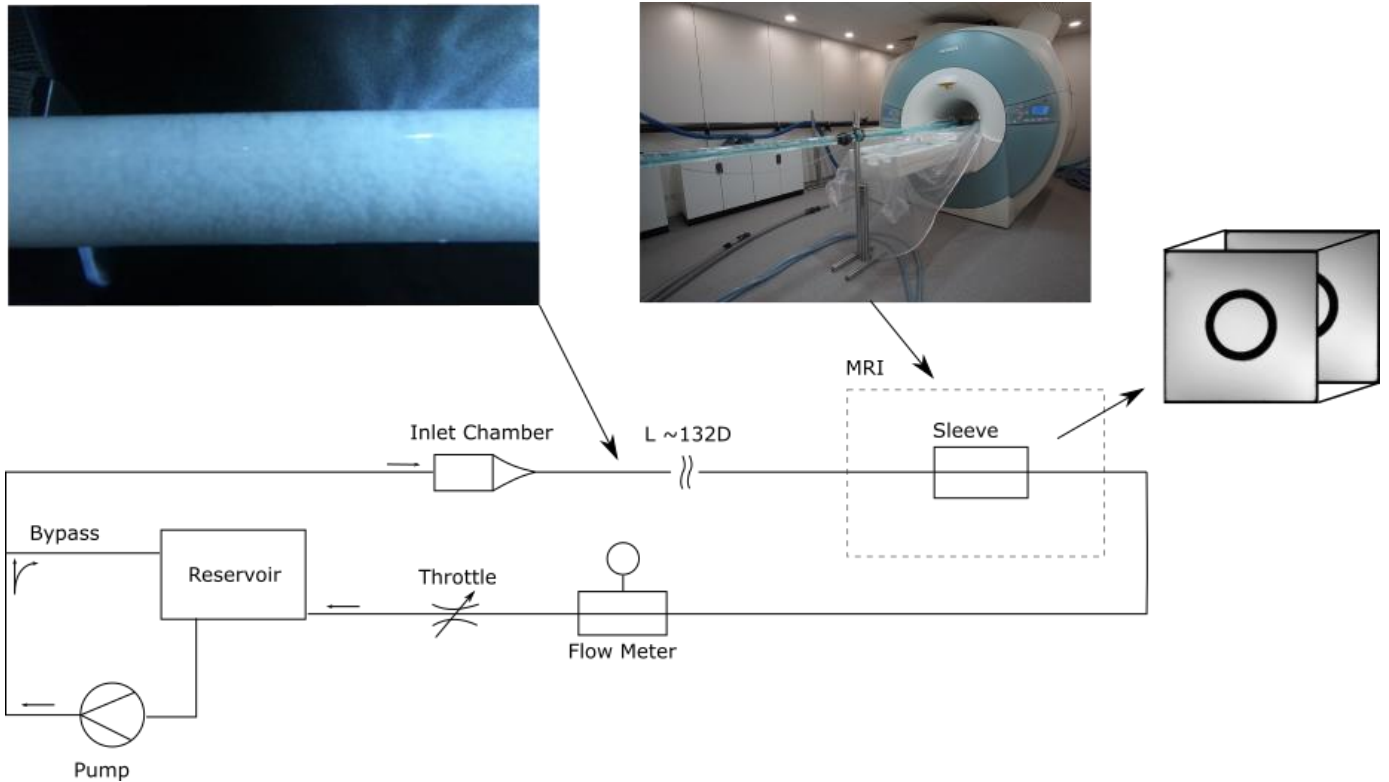


Fig. 1: Schematic of the experimental setup, including some pictures of the measurement campaign. A rectangular box (sleeve), filled with static liquid, was used for the magnetic drift correction as shown in Eq. (1).

The MRV measurements were conducted on a Siemens 3T Magnetom Tim Trio (Siemens, Erlangen, Germany). The applied pulse sequence is a basic Gradient-recalled echo sequence with velocity encoding. To take advantage of the symmetry of the flow system, the voxel size was set to 50 mm in the direction of the pipe axis. The voxel size in the cross-sectional plane was 0.3 mm \times 0.3 mm. With this anisotropic resolution, the voxel volume is increased by a factor of 16.7 compared to the case when an isotropic voxel of size $(0.3 \text{ mm})^3$ was selected. The measurement uncertainty, which is inversely proportional to the voxel volume, is thereby greatly reduced for the same measurement time. In addition, spatial averaging reduces signal ghosting, which, as explained in the previous section, is caused by transient flow effects. Compared to isotropic voxels, the anisotropic voxels in the fully-developed flow contain a larger range of time scales, which reduces signal ghosting.

Each two-dimensional acquisition contained 640 \times 640 voxels in the cross-sectional plane and was averaged 32 times to further reduce measurement uncertainty. The k-space was sampled line by line with a sampling duration of 3.5 ms for each line. The total acquisition time was just under 30 minutes. For comparison, the expected time scales in the flow, which can be estimated with the

pipe diameter and the bulk velocity, do not exceed 0.3 s. Hence, the results are expected to have fully converged statistically.

The local particle concentration was determined from the signal magnitude M of a measurement with particles and a reference magnitude M_{ref} of a measurement without particles. Since the two measurements were separated by several hours, it was necessary to correct a possible temporal drift of the signal magnitude. The drift was measured in a rectangular sleeve with static fluid as shown in Fig. 1. Finally, the local particle concentration φ was calculated with

$$\varphi(x, y) = 1 - \frac{M(x,y)/\overline{M_{sleeve}}}{M(x,y)_{ref}/\overline{M_{sleeve,ref}}} \quad (1)$$

where $\overline{M_{sleeve}}$ and $\overline{M_{sleeve,ref}}$ is the average signal magnitude in the sleeve of the measurement with particles and without particles.

3. Results

Figure 2 shows the qualitative particle concentration obtained with Eq. (1) for some of the investigated cases. The parameters Φ and Re are the target mean particle concentration and the target suspension Reynolds number, respectively. Here, blue pixels show a low particle volume fraction and green pixels show a high particle volume fraction. Note that the theoretical maximum lies at $\varphi(x, y) = 64\%$ which is the highest average volume fraction that can be occupied by randomly packed monodisperse hard spherical particles. This number is exceeded near the pipe center for the measurements depicted in the bottom row in Fig. 2, which can be explained as an effect of the polydispersity (statistical variations in diameter) of the particles resulting in higher packing densities (Farr, 2013). Also, it can be seen that the concentration distribution is slightly asymmetrical for measurements up to a mean concentration of $\Phi = 0.2$, which is a result of small density differences between the fluid and particles. These density changes are due to minor temperature variations.

These buoyancy effects diminish for the higher particle concentrations. For $\Phi > 0.2$, multiple concentric rings appear between the high particle concentration region near the pipe center and the pipe wall.

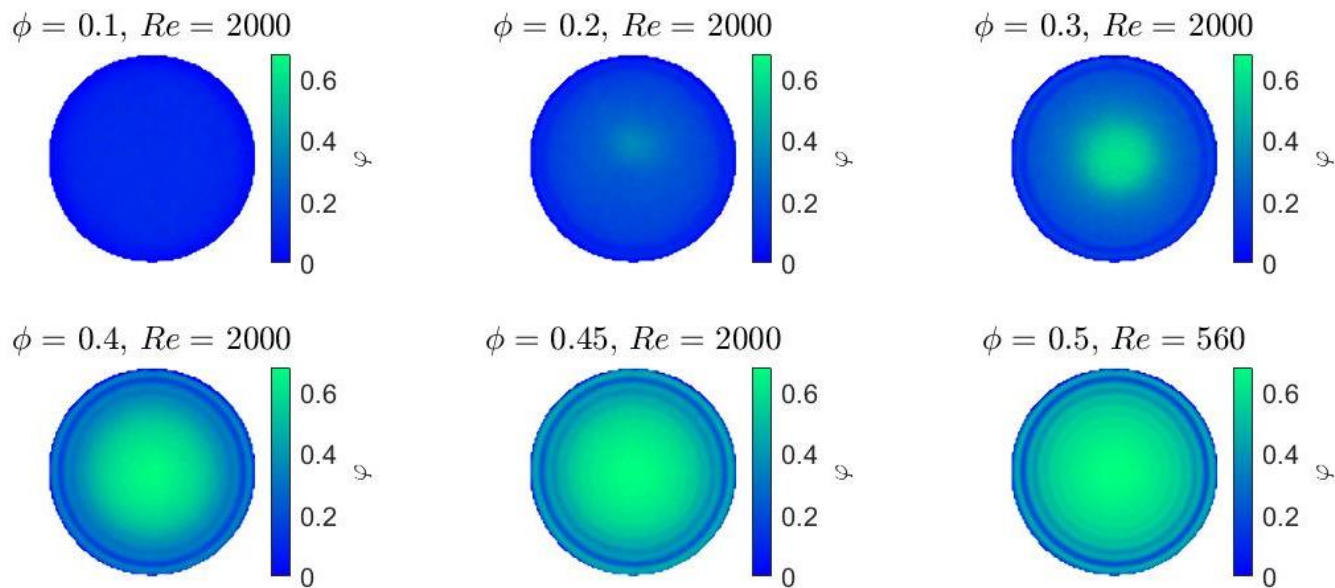


Fig. 2: Contour plots of the time-averaged local particle volume fraction.

Figure 3 shows the quantitative particle concentration for the target Reynolds numbers 800, 2000 and 5000. Note that the figure also includes data with $\Phi = 0.5$ and $Re = 560$, which was the maximum Reynolds number that was reached with this high particle concentration. With this case, a minimum of five ring structures can be seen in the data.

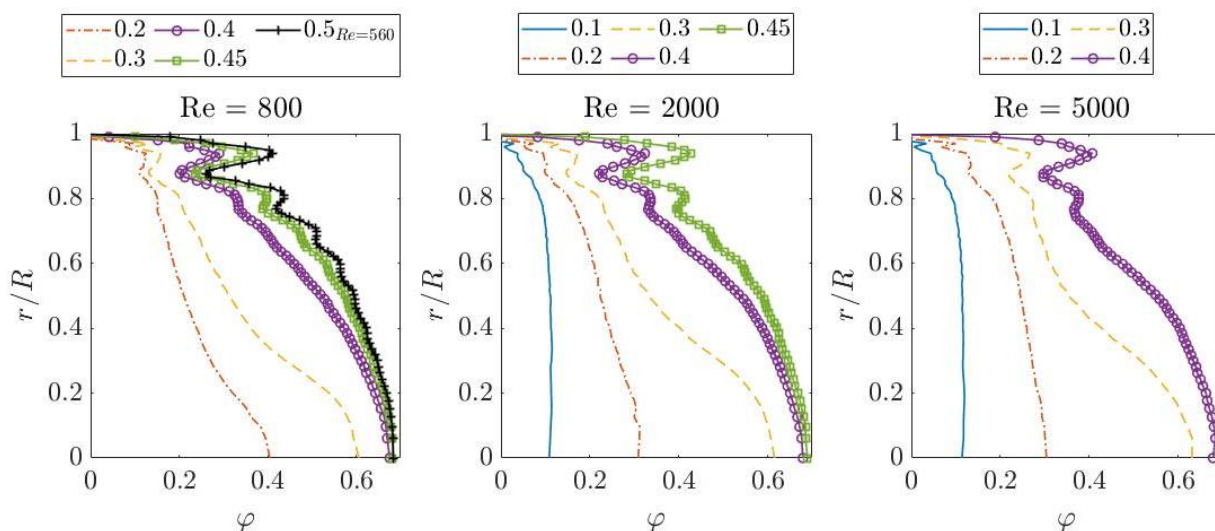


Fig. 3: Profiles of the time-averaged local particle volume fraction for three target Reynolds numbers.

Figure 4 shows the time-averaged velocity profiles obtained with the velocity encoded MRV sequence. It can be seen that high particle concentrations result in a flatter velocity profile. Even at low Reynolds numbers, which corresponds to a laminar flow for the single-phase case, a distinctively flat profile appears for $\Phi > 0.3$. The position of these velocity plateaus correspond to regions with an exceptionally high local particle concentration, see Fig.3.

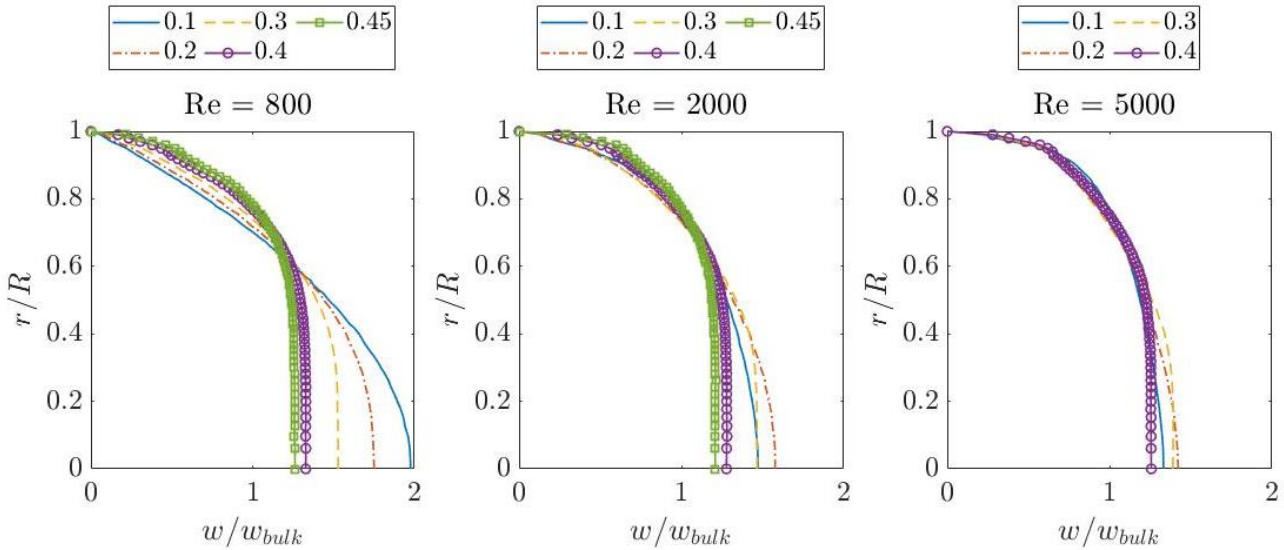


Fig. 4: Profiles of the non-dimensional time-averaged intrinsic fluid velocity in the stream-wise direction for three different target Reynolds numbers and various target particle concentrations.

Overall, the most striking behavior observed in this study are the ring-like structures in the particle concentration. To the best of the authors' knowledge, the occurrence of multiple rings has not been well researched. These rings are most likely caused by the limited movement in radial direction. Essentially the particles are trapped between the center and the wall, which result in the formation of these rings starting at the pipe wall. The number of rings and their appearance seem to depend on the mean particle concentration and are only slightly influenced by the Reynolds number

4. Conclusion

This study demonstrates the capabilities of MRV measurements in particle-laden flows. The results agree with the general trends described in the literature (e.g., Matas et al., 2003, Hogendoorn & Poelma, 2018). Furthermore, it was observed that multiple ring-like structures form once a certain particle packing in the center is reached. The on-going study focuses on turbulence measurements in these flows to further examine the observed behavior. An MRV technique for Reynolds stress tensor measurements in particle-laden flows is currently being developed. In addition, direct numerical simulations are performed in order to validate the

obtained results. This will also shed light on the observed phenomena and will unveil the responsible underlying mechanisms.

References

- Eilers, V. H. (1941). Die viskosität von emulsionen hochviskoser stoffe als funktion der konzentration. *Kolloid-Zeitschrift*, 97(3), 313-321.
- Farr, R. S. (2013). Random close packing fractions of lognormal distributions of hard spheres, *Powder Technology*, 245, 28-34
- Hogendoorn, W., & Poelma, C. (2018). Particle-laden pipe flows at high volume fractions show transition without puffs. *Physical review letters*, 121(19), 194501.
- Poelma, C. (2020). Measurement in opaque flows: a review of measurement techniques for dispersed multiphase flows. *Acta Mechanica*, 231(6), 2089-2111.
- Matas, J. P., Morris, J. F., & Guazzelli, E. (2003). Transition to turbulence in particulate pipe flow. *Physical review letters*, 90(1), 014501.